



## FINAL TECHNICAL REPORT

PALEOSEISMIC INVESTIGATIONS OF HOLOCENE EARTHQUAKE  
RECURRENCE ON THE PENINSULA SEGMENT OF THE SAN  
ANDREAS FAULT, WOODSIDE, CA:

*COLLABORATIVE RESEARCH WITH FUGRO WILLIAM  
LETTIS&ASSOCIATES AND THE UNITED STATES GEOLOGICAL  
SURVEY , JOINT PROJECT WITH JUDY ZACHARIASEN, URS  
CORPORATION*



*Prepared for*  
U.S. Geological Survey  
National Earthquake Hazards Reduction Program  
Award Numbers 06HQGR0195 and G09AP00048

August 2011



**FINAL TECHNICAL REPORT**

**PALEOSEISMIC INVESTIGATIONS OF HOLOCENE EARTHQUAKE  
RECURRENCE ON THE PENINSULA SEGMENT OF THE SAN ANDREAS  
FAULT, WOODSIDE, CA: COLLABORATIVE RESEARCH WITH FUGRO  
WILLIAM LETTIS&ASSOCIATES AND THE UNITED STATES  
GEOLOGICAL SURVEY, JOINT PROJECT WITH JUDY ZACHARIASEN, URS  
CORPORATION**

**Principal Investigators:**

John N. Baldwin and Özgür Kozacı, Fugro William Lettis and Associates, Inc.  
(Award 06HQGR0195)  
1777 Botelho Dr., Suite 262, Walnut Creek, CA 945961  
(tel: 925-256-6070; fax: 925-256-6076  
j.baldwin@fugro.com, o.kozaci@fugro.com

Judith Zachariasen, URS Corporation  
(Award G09AP00048)  
1333 Broadway, Suite 800, Oakland, CA 94612  
(510) 874-1749 (phone); (510) 874-3268 (fax);  
judy\_zachariasen@urscorp.com

Carol Prentice, U.S. Geological Survey  
345 Middlefield Road, M.S. 977, Menlo Park, CA 94025  
650-329-5690 (phone); 650-329-5163 (fax)  
cprentice@usgs.gov

**Program Elements I and III  
Northern California Region**

**Keywords:**

Quaternary fault behavior, neotectonics, paleoseismology

U. S. Geological Survey  
National Earthquake Hazards Reduction Program  
Award Number 06HQGR0195

August 2011

This research was supported by the U.S. Geological Survey (USGS), Department of the Interior, under USGS Awards 06HQGR0195 and G09AP00048. Term of the 06HQGR0195 award was 1 August 2006 to 31 July 2011. The views and conclusions contained in this document are those of the Principal Investigators only and should not be interpreted as necessarily representing the official policies, either expressed or implied, of the U.S. Government.



## ABSTRACT

The Peninsula section of the San Andreas Fault is a significant hazard for the San Francisco Bay area, but the earthquake history of the San Andreas fault through the San Francisco peninsula region remains enigmatic. Little is known about the timing of earthquakes on this section of the fault prior to the great earthquake of April 18, 1906. An earthquake in 1838, with an estimated magnitude between M6.8 and 7.4, produced strong shaking on the San Francisco Peninsula, and most workers have assumed that this event occurred on the San Andreas fault. However, paleoseismic excavations across the fault at several sites on the Peninsula have failed to provide evidence that the 1838 earthquake was associated with surface rupture on the San Andreas fault. The lack of a robust paleoseismic history means that the seismic hazard posed by the northern San Andreas fault to the San Francisco Bay Area is poorly understood - does the fault rupture only in large 1906-style events, or also in smaller, localized events, perhaps limited to the Peninsula or smaller sections? In this study, we have aimed to address the lack of a well-constrained earthquake history by acquiring paleoseismic data from trenches at the Crystal Springs South site on the Peninsula section, near Woodside, CA.

We used LiDAR images produced from data collected by the GeoEarthScope project to search for promising paleoseismic sites along the Peninsula section of the San Andreas fault. At a site about 1.2 km southeast of Crystal Springs Reservoir, we excavated two trenches across the fault and exposed fluvial gravel and floodbank deposits overlying an older weathered, clay-rich colluvial unit. The oldest dated fluvial deposits are on the order of 1000 years old; the underlying colluvium is about 3100 years old. The fluvial deposits have been cut by two distinct generations of faults. The younger set of faults break nearly to the ground surface, and we interpret these to represent 1906 surface faulting that has been buried by post-1906 sediments. The older faults terminate below a colluvial wedge derived from one of the fluvial gravel deposits. The scarp-derived colluvium overlies a faulted fine-grained overbank deposit that in turn rests on the channel gravel, and represents the ground surface at the time of the older earthquake. The scarp-derived colluvium is overlain by a fine-grained overbank deposit. The older event, marked by the presence of a colluvial wedge sandwiched between dated overbank deposits, likely occurred between about 600 and 1000 years ago.

The record of two earthquakes in 1000 years is similar to the paleoseismic record at the Crystal Springs site to the northwest. In contrast, at Portola Valley to the southeast, evidence of three to four events in 1000 years was observed. As at these other sites, there is no evidence at the Crystal Springs South site of the postulated 1838 earthquake. The long interval between the 1906 and penultimate events at the Crystal Springs and Crystal Springs South sites, and the difference between the records there and at other sites along the Peninsula and Santa Cruz Mountains segments, call into question preferred seismic hazard models in which the entire San Andreas fault ruptures together, similar to the 1906 rupture. It may be as or more common that different parts of the fault rupture independently, yielding different rupture histories at different locations.



## TABLE OF CONTENTS

Final Technical Report.....	1
1.0 Introduction.....	1
2.0 Previous Work .....	3
2.1 1906 Earthquake .....	3
2.2 Paleoseismic Studies.....	3
3.0 Crystal Springs South (CSS) Site.....	5
3.1 Setting .....	5
3.2 Methods.....	5
3.3 Trench Stratigraphy .....	5
3.3.1 Trench T2 .....	6
3.3.2 Trench T1 .....	8
3.4 Age Constraints.....	9
4.0 Discussion.....	12
5.0 Conclusions.....	14
6.0 Acknowledgments.....	15
7.0 References.....	17



## LIST OF TABLES AND FIGURES

**Table 1.** Radiocarbon Data from Crystal Springs South Trenches 1 and 2, August 2010

**Figure 1.** Map of the northern San Andreas fault system, including the Peninsula segment (SAP). From WGCEP (2003).

**Figure 2.** (2003) map of the Peninsula (SAP) and adjacent segments.

**Figure 3.** San Andreas fault Peninsula segment near Woodside, CA.

**Figure 4.** Alternative reconstructions of channel offset from the Filoli paleoseismic site.

**Figure 5.** Site map. Bare earth DEM obtained from LiDAR data of Crystal Springs South site.

**Figure 6.** Photograph of trench site.

**Figure 7a.** Log of southeast wall of Trench 2.

**Figure 7b.** Log of northwest wall of Trench 2.

**Figure 8.** Log of northwest wall of Trench 1.

**Figure 9.** Close-up of the fault zone in the southern wall of Trench T2 with radiocarbon samples.





## 1.0 INTRODUCTION

The northern San Andreas fault last ruptured in the 1906 M 7.9 San Francisco earthquake along its full extent from the northern end of the creeping segment near San Juan Bautista to Shelter Cove near the Mendocino triple junction (Figure 1). The Working Groups on California Earthquake Probabilities (2003, 2008 hereinafter referred to as WGCEP, 2003, 2008), building on models of previous working groups (e.g. WGCEP, 1988, 1990; WGNCEP, 1996), divided the northern San Andreas fault into four segments, which differ from one another in one or more characteristics such as average strike, slip rate, recurrence interval, and age of penultimate earthquake. These segments, from north to south, include Offshore (SAO), North Coast (SAN), Peninsula (SAP), and Santa Cruz Mountains (SAS) (Figure 1). This segmentation reflects the idea that some earthquakes on the northern San Andreas fault may result from rupture of only a section of the fault, in addition to earthquakes generated by multi-segment rupture of the NSAF similar to 1906. WGCEP (2003) developed assessments of earthquake probability on the San Andreas fault based on interpretations of the data and expert opinion regarding the mode of failure of paleo- and ostensibly future earthquakes. These assessments are highly dependent on estimates of the likelihood that multi-segment ruptures are more or less common than single-segment ruptures. Such estimates are themselves highly dependent on the rupture behavior of past earthquakes and thus on the paleoseismic record on different segments and indeed along the length of the fault. To date, the paleo-earthquake record on the northern San Andreas is incomplete, with few paleoseismic sites recording more than a small number of events. Thus, a key element to improving the assessment of northern San Andreas earthquake probabilities is to improve the paleoseismic record so as to test different models of segmentation and coseismic rupture. This study has addressed this issue by providing further paleoseismic data on the Peninsula segment, a segment that currently has an extremely limited record of paleoearthquakes.

The Peninsula segment as defined by the WGCEP (2003) is about 85 km long and extends from the Golden Gate southward to the north end of the Loma Prieta aftershock zone (WGNCEP, 1996; 2003; Figure 2). It is flanked to the north by the North Coast segment and to the south by the Santa Cruz Mountains segment (Figure 1). The northern end of the Peninsula segment coincides with the junction of the San Gregorio fault and the San Andreas fault. Average slip in the 1906 earthquake also decreased south of the Golden Gate from about 5 m to about 3 m. The southern end of the segment coincides with a restraining bend in the fault and a lithologic change.

The working groups have used historical and paleoseismic characteristics to define rupture models based on these segments that include scenarios involving rupture of the full length of the fault (e.g. 1906 earthquake) and rupture of one, two, or three segments. The extent to which segment boundaries defined by geologic characteristics actually represent constraints on individual earthquake ruptures remains uncertain, but they have nevertheless formed the basis for the working groups' seismic source characterization and hazard assessment. WGCEP (2003) and WGCEP (2008) prefer rupture models that involve failure of the entire northern San Andreas fault, as in 1906, based on similar ages for some events observed at paleoseismic sites on the SAS and SAN segments, which have been inferred to be the same event. However, the timing of some past events at paleoseismic sites on the SAS differs from that on other sections, suggesting that at least some earthquakes involve smaller ruptures. WGCEP (2003) and WGCEP (2008) favor a rupture model in which those smaller events involve rupture of SAS and SAP together rather than independently. The result of the working group assessments is that seismic hazard from the northern San Andreas fault is dominated by larger, more infrequent events. This result is strongly dependent on assumptions about behavior of the Peninsula segment that is poorly constrained by paleoseismic data. There is no site on the Peninsula segment to date with a well-developed event



chronology. If the Peninsula were shown to have a very different recurrence from segments to the north and south, smaller segment ruptures would become commensurately more significant in the fault model and the hazard could be very different, with a greater contribution from smaller but more frequent earthquakes. In order to assess the validity of the seismic hazard model, it is crucial that a robust paleoearthquake record be developed on the peninsula.

The age and extent of the penultimate event on the Peninsula segment is unknown, and constraints on older events are minimal to nonexistent. Modeling of intensity data by Topozada and Borchardt (1998) and Bakun (1999) indicates that the 1838 historical earthquake, which has magnitude estimates of  $M$  6.8-7.4, was located on the peninsula. The San Andreas fault has been proposed as the likely fault, but direct evidence for the event on the SAP is lacking. Hall et al. (1999) interpreted offsets of stream channels at the Filoli paleoseismic site (Figure 3) to indicate a pre-1906 earthquake that occurred after deposition of deposits dated to AD 1420-1820 (discussed in more detail below). The inferred slip in that event was about 60% of that in 1906, leading them to conclude that the penultimate event ruptured a shorter length of the fault, possibly only the Peninsula segment. They tentatively equate this paleoearthquake with the 1838 earthquake, but, whereas it is a plausible explanation, there is no direct evidence that the two events are one and the same. Recent paleoseismic work on the Peninsula segment at the Crystal Springs and Portola Valley sites (Figure 3) reveals no evidence for the 1838 earthquake (Baldwin et al., 2006; Prentice and Moreno, 2007; Prentice et al., 2008; Sundermann et al., 2008). Nevertheless, the tentative interpretations of inconclusive data from Filoli have been part of the basis for segmentation and rupture modeling of the northern San Andreas fault and consequently for the assessment of seismic hazard posed by the fault to the San Francisco Bay Area.

In this report, we present results of a new paleoseismic study at the Crystal Springs South site, just north of Filoli, which is providing further information about the age of the penultimate event on the Peninsula segment (Figure 3).



## 2.0 PREVIOUS WORK

### 2.1 1906 Earthquake

The Lawson report (Lawson, 1908), which documented surface displacements that occurred along the San Andreas fault during the 1906 earthquake, reports offsets to the north and south of the Crystal Springs South site. The nearest site to the north is at the causeway between Upper and Lower Crystal Springs reservoirs, about 4.7 km northwest of the site. The offset of the causeway was reported to be 8 ft (about 2.4 m). To the south, between Woodside and Portola Valley, about 9 km southeast of the site, J.C. Branner observed two fences offset about 8 and 8.5 ft (about 2.4 and 2.7 m). In Portola Valley, farther south, the documented slip dropped considerably. Rows of prune trees were reported to be offset about 2 ft (0.6 m). Reassessment of the photographs of this site suggested the total offset was about 1.2 m (Hall et al., 2001).

### 2.2 Paleoseismic Studies

Whereas the North Coast and Santa Cruz segments of the San Andreas fault each have paleoseismic sites that have yielded multi-event paleoseismic records, the Peninsula segment has seen only limited work to date, none of which, unfortunately, has yielded a robust history.

The nearest paleoseismic site to the Crystal Springs South site is at the Filoli estate, about 0.5 km to the southeast. At the Filoli site (Figure 3), Hall et al. (1999) excavated numerous fault-perpendicular and fault-parallel trenches where Spring Creek had breached the San Andreas fault scarp and deposited late Holocene alluvial fan materials over the fault. They obtained the currently accepted best estimate for Holocene slip rate on this segment,  $17 \pm 4$  mm/yr, from the  $30 \pm 2$  m offset of the thalweg of a channel dated to  $2070 \pm 120$  BP.

Efforts to develop a robust event chronology at the Filoli site were relatively unsuccessful due to the coarse and discontinuous nature of the channel deposits. Hall et al. (1999) did, however, infer the occurrence of two late Holocene earthquakes from a series of channels. The youngest suite of nested channels was offset about 2.5 m, which they concluded occurred during the 1906 earthquake because of its similarity in slip to that measured nearby following the event. A second set of nested channels was found deeper in the section. Hall et al. (1999) cut back the fault-parallel trench walls to within a few meters of the fault and projected the channels into the fault on either side. Based on their projections, they concluded the older channel sequence was offset about  $4.1 \pm 0.5$  m. The channel deposits were dated to  $330 \pm 200$  BP (1476-1647 AD calendar age). Because this offset was greater than the offset of the youngest channel sequence, they inferred that that this set of channels had been offset in the 1906 and the penultimate earthquakes and, thus, that the penultimate earthquake had occurred after  $330 \pm 200$  BP. Furthermore, because the estimated offset of about  $1.6 \pm 0.7$  m in that event was smaller than the ca. 2.5 m that occurred in 1906, they concluded that the earthquake was likely generated by rupture of a shorter section of fault than in 1906, perhaps only the Peninsula segment, and probably had a magnitude of about **M** 7.0-7.4. They suggested, based on the poorly constrained age of the event and their inferences regarding rupture length, that the 1838 earthquake, which occurred on the peninsula, was a candidate for the event. Although they and others merely proposed the 1838 event as a possible candidate, this proposal has taken on a life of its own, and the 1838 event is now regularly considered to have resulted from rupture of the Peninsula segment of the San Andreas fault. The assignment of a date of 1838 to the penultimate event at Filoli, however, remains speculative. Furthermore, the channel offset data allow



alternative interpretations, including that there is no additional offset of the older channel (Figure 4; Zachariassen et al., 2010). Thus no pre-1906 event is required to explain the data at the site.

Hall et al. (1999) also speculated on the occurrence of the third event back. The older channel sequence described above, which crossed the fault at high angle, looped back and ran along the fault for about 25 m. They suggested that a stream is most likely to begin following a fault immediately after a surface rupturing event. Thus, they speculate that the prior event occurred shortly before the age of deposition of the channel deposits. Thus, they surmised that the age of the third event was during or shortly after ca. 1467-1647 AD. Again, however, this was purely speculative, and their study provided no direct evidence of the third event at Filoli.

In recent years, further paleoseismic efforts have been directed towards the Peninsula segment, which have produced mixed results. Prentice and Moreno (2007) excavated a trench in alluvial fan deposits at the north end of Crystal Springs reservoir, about 10 km northwest of the Crystal Springs South site, and identified the 1906 rupture and one prior event. The age of the prior event was not reported but the absence of European pollen in sediments bracketing the event horizon suggests the event predates the 1820 European settlement. More recent age constraints suggest the event occurred between AD 890-1260 (Prentice et al., 2008). Another trench at Crystal Springs reservoir exposed evidence of the 1906 earthquake but no earlier events in the upper 3 m (since ca. AD 1130 [Prentice et al., 2008; C. Prentice, pers. comm., 2008]). Prentice et al. (2008) suggest possible explanations for these observations including (1) that all exposed deposits postdate the penultimate event because of high sedimentation rates; (2) a long elapsed time between earthquakes, or (3) the event horizon represents multiple earthquakes, not just 1906.

Baldwin et al. (2006) and Baldwin and Prentice (2008) report evidence of two or three pre-1906 events in about 1000 years exposed in a trench at Portola Valley Town Center. These events have been interpreted from warped marsh/fluvial and colluvial wedge stratigraphy. The interpretation includes events occurring at: A.D. 1030 to 1490, A.D. 1260 to 1490, and 1906; interpreting the second event as two events (AD 1260-1490 and AD 1410 to 1640) is also permitted by the data (Baldwin and Prentice, 2008). The stratigraphy is complicated and the results depend on preservation of per-event colluvial wedges, which may or may not be reflected in a complete earthquake record. Evidence for an 1838 event was not found, but the resolution is not sufficient to rule it out.

The penultimate event identified at Grizzly Flat, on SAS, southeast of the Peninsula segment, has been dated to AD 1630-1660 (or 1600-1670; Schwartz et al., 1998); the penultimate event at Vedanta, on SAN, northwest of the Peninsula, occurred between AD 1670 and 1740 (Zhang et al., 2006). The similarity in penultimate event ages at these sites, and also Bolinas Lagoon (Knudsen et al., 2002), has been used to support a full-fault rupture interpretation for the penultimate event on the northern San Andreas fault (Schwartz et al., 1998). Conversely, these could be independent smaller events closely spaced in time. WGCEP (2003, 2008) preferred the former model. Determining the age of the penultimate and earlier events on the Peninsula segment would be significant in evaluating the two models.



### 3.0 CRYSTAL SPRINGS SOUTH (CSS) SITE

#### 3.1 Setting

This study presents the results of a trenching investigation of the CSS paleoseismic site, between Filoli and Crystal Springs reservoir (Figures 1, 5 and 6). The site is in the San Francisco Public Utilities Commission (SFPUC) Peninsula Watershed. We selected the site using the UNAVCO Plate Boundary Observatory Earthscope LiDAR data, acquired along the full length of the northern San Andreas fault (Figure 5).<sup>1</sup> At this site, the San Andreas fault runs along the eastern edge of the Santa Cruz mountains, along the western edge of the fault-controlled San Andreas “rift” valley. The fault here has a component of west-side-up vertical displacement, which has led to the formation of a 5-10 m-high scarp along the foot of the mountains. The setting is similar to that of the Filoli site, in that Holocene sedimentation has been dominated by deposition of alluvial deposits from Spring Creek. The creek, which is currently entrenched to the south of the site, has breached the scarp and deposited alluvium across and east of the fault. The fault here strikes about N35W. We selected the CSS site where the main fault scarp has been eroded back, leaving the fault itself outboard of the eroded scarp and buried by young alluvial deposits from Spring Creek. A small Holocene scarp is evident in the LiDAR data and on the ground, just north of the intersection of Old Cañada Rd. and a small spur road heading northeast (Figure 5). Trench T1 was excavated across the Holocene scarp; trench T2 is located to the southeast, on the south side of the spur road, on strike with the Holocene scarp but where the fault is buried and no scarp is readily evident in the Lidar or on the ground (Figure 6).

#### 3.2 Methods

The trenches were excavated with a rubber-tire backhoe with a 3-foot bucket and shored with 7-foot aluminum hydraulic speed shores. Topsoil was stored separately from the remaining spoil, which was covered with tarps. All spoil was stored on plywood sheets in order to minimize impact to the ground surface, and a wildlife exclusion fence was erected around each trench. Biological, cultural, and Native American monitors provided by the SFPUC over saw the excavation. The trench walls were manually scraped and cleaned, then gridded with a 1- by 0.5 m string grid. We produced sketch logs of each wall on mylar graph paper at 1:20 scale. We photographed each grid square, rectified the photographs in ArcGIS 9.3, and created rectified photomosaics of each wall in Adobe Photoshop. Detailed logging was then done on the photologs at 1:15 and 1:12 scale for Trench T1 and T2, respectively. We collected charcoal samples for radiocarbon dating as well as bulk soil samples and samples for pollen analysis.

#### 3.3 Trench Stratigraphy

Both trenches exposed fluvial channel and overbank deposits that overlie a dark grey clayey deposit that contains completely weathered pebble-sized clasts; this is the deepest deposit exposed in the trenches and is likely older, highly weathered colluvium. The overlying fluvial deposits are cut by two distinct generations of faults. The younger set of faults break nearly to the ground surface, and we interpret these

---

<sup>1</sup> This material is based on services provided to the Plate Boundary Observatory by NCALM (<http://www.ncalm.org>). PBO is operated by UNAVCO for EarthScope (<http://www.earthscope.org>) and supported by the National Science Foundation (No. EAR-0350028 and EAR-0732947). This material is provided by the OpenTopography Facility (<http://www.opentopography.org>) with support from the National Science Foundation under NSF Award Numbers 0930731 & 093064.



to represent 1906 surface faulting that has been buried by post-1906 sediments. The older faults terminate below colluvial rubble derived from faulted gravel deposits. Descriptions of each trench follow.

### **3.3.1 Trench T2**

Stratigraphic and faulting relationships are clearest in trench T2, especially the south wall (Figures 7a and 7b). The trench was excavated northeast-southwest, across and orthogonal to the southeastward projection of the Holocene scarp observed north of the spur road (Figure 5). The trench was about 8 meters long and 2-2.5 m deep. The depth was limited by the presence of ground water, which was somewhat shallower on the west side of the fault. The fault zone is located between vertical meters 4 and 6 in the trench.

The trench exposed a suite of fluvial deposits overlying old weathered colluvium (unit 100). The basal unit was evident from about 1 m above the trench floor on the west side of the fault. On the east side it was at or just below the floor of the trench; we exposed the upper surface at several locations along the floor. It is light to dark grey, often with orange mottling, sandy silty clay to clayey sand and contains scattered to abundant, highly to completely weathered pebbles that can be scraped away with a tool. The uppermost part of the deposit is coarser, primarily clayey sand, darker and more organic-rich, with less mottling. The dark grey color at the top may represent a paleosol. From about meter 3.5 eastward, in the southeast wall, the color transition between dark grey and orange mottled grey follows the upper contact and bends down into the floor of the trench (Figure 7a). Although the transition is abrupt and subparallel to the faults that occur to the east, we found no evidence that it was a fault contact. The color change may be due to groundwater conditions or wetting and drying along the edge of the channel that eroded into it.

Fluvial deposits overlie the basal colluvium. The upper contact of the colluvium is generally eroded and scoured, suggesting the stream removed an unknown amount of the colluvium prior to depositing the alluvium. We have divided the fluvial deposits into large packages based on the relative amounts of fine vs. coarse-grained materials, but each large package contains numerous lenses of material with different grain sizes, and many of the contacts are gradational. Directly overlying the weathered colluvium is a channel gravel unit (unit 60). This is a largely clast-supported granule to cobble gravel in a dry, loose sand to granule matrix. Clasts are subrounded to rounded and reach about 10 cm. Crude bedding is present in places and numerous lenses of silt and sand are present. Unit 60 is about 20 cm thick at the western end of the trench but deepens into a channel of greater than a meter thickness. This channel is cut by the fault where it is thickest. Unit 60 is present on both sides of the fault.

Above the gravel deposit is a fine-grained overbank deposit of sand and silt (Unit 40), with several small lenses of granule to pebble gravel; coarser gravel lenses occur at the western end of the trench. It is dry, hard, yellow to tan, primarily sandy silt but with gradational transitions to primarily sand and occasional concentrations of more clay-rich silt. It contains abundant roots, charcoal and krotovina. Between meters 1 and 2 in the southeast wall and between meters 6 and 8 in the northwest wall, paleosols have developed (Figures 7a and 7b); they are likely not correlative. This unit is present along the full length of the trench. Within the fault zone, we have been able to subdivide unit 40 into smaller subunits; these are not readily evident outside the fault zone. In the southeast wall, these subunits consist, from bottom to top, of: C) sand, B) sandy pebble gravel, and A-A') silty sand to fine sandy silt (Figure 7a). In the northwest wall, a clean sand (subunit a) underlies silty sand with pebbles (b; b\* has higher concentration of pebbles) (Figure 7b). The uppermost subunit of 40 in the northwest wall is a sandy silt (c).

A gravel unit (Unit 25) overlies the unit 40 silt on the east side of the fault only. This well-sorted, matrix-



to clast-supported gravel contains smaller, somewhat less rounded clasts than the lower unit 60 channel gravel. Clasts are generally pebble to granule sized and are coarser near the fault zone, becoming smaller eastward. On the north wall exposure, this unit contains a greater concentration of fine-grained material, primarily occurring as lenses within the gravel. This gravel was likely deposited by a stream flowing at the base of the fault scarp, leaving deposits only on the downthrown side of the fault.

The uppermost deposits (units 20 and 10) in the trench comprise heavily bioturbated yellow-brown, hard, dry, massive pebbly sandy silt. It appears colluvial but the extensive bioturbation has removed evidence of any bedding or structure that would clarify its origin. It contains abundant roots and charcoal. The uppermost part of this (unit 10) includes the modern A-horizon.

Within the fault zone, between meters 4 and 6, there is also present a unit labeled "R" in figures 7a and 7b. This unit, which is found between subunits of unit 40, includes unsorted, unbedded, chaotic, pebble to cobble gravel with abundant silt and sand. We interpret this to be a colluvial wedge of rubble derived from unit 60, which was exposed during faulting, providing a source for the gravel. A classical wedge shape is evident on the south wall exposure (Figure 7a); on the north wall (Figure 7b), the wedge is not clear and the material appears as an irregularly shaped deposit of rubble. This is discussed further below.

#### Event Stratigraphy

The fault zone in trench T2 is about one and a half meters wide and includes evidence of two distinct events. The youngest event is represented by the faults that reach highest in the section; these are marked in red in Figures 7a and 7b. This generation of faults, which occur on either edge of the fault zone, terminate within the bioturbated material near the top of the trench (unit 20). Because of the bioturbation, the exact termination has been obscured. Nevertheless, all these faults can be followed to approximately the same stratigraphic horizon within this zone and appear to affect the same deposits. They affect the unit 40 silt and sand and all or most of the unit 20 bioturbated sandy silt. We interpret these faults to represent traces of the 1906 rupture.

A second event, which we call "Event G", is evident in the stratigraphy and is represented by the faults that are colored purple in Figures 7a and 7b. The scarp-derived colluvium "R" occurs within the fine overbank deposits of Unit 40. It overlies faulted overbank deposits (Unit 40, subunit A in the southeast wall [Figure 7a] and subunit b in the northwest wall [Figure 7b]), which constituted the ground surface at the time of the older earthquake (Event G on Figure 7a). The scarp-derived colluvium is in turn overlain by more fine-grained material. We interpret the stratigraphy to indicate that the earlier event occurred when Unit 40 was at the ground surface and overbank silts were being deposited. Because only the lower part of Unit 40 had been deposited at the time of the event, the underlying gravel (Unit 60) was exposed in the scarp. Gravel fell from the exposed scarp and was deposited on the overbank sands and silts of lower Unit 40 (subunit A, silty sand). The fluvial environment did not change significantly following the event, and silt overbank deposition continued (unit A', fine silty sand, the post-event deposit is similar to A, the pre-event deposit, though slightly finer. Thus, the colluvial wedge from the penultimate event is sandwiched between earlier and later Unit 40 overbank deposits. These relationships are well expressed in the south wall of the trench (Figure 7a). In the north wall (Figure 7b), the relationships are less clear, in part because the younger (1906?) event faulted through the older fault zone and colluvium. Rubble from the penultimate colluvium has been drawn into the fault zone of the 1906 event, overprinting the earlier event and leaving the stratigraphic and faulting relationships less clear.

There is no evidence in the trench for any other event since the start of deposition of the fluvial deposits



that overlie the dark basal clay-rich material.

### 3.3.2 Trench T1

Trench 1 trends northeast, orthogonal to the fault and was excavated across the small west-side-up scarp evident in the Lidar and on the ground. The trench is about 12 meters long and 2-2.5 m deep. The fault zone is below the scarp, between meters 6 and 8. The east side is downthrown relative to the west side. The log of the north wall of the trench is shown in Figure 8.

The stratigraphy in Trench 1 is broadly similar to that in Trench 2. The same grey clay-rich weathered colluvium (unit 100) forms the basal unit. On the west end of the trench, this unit is a massive, light brown, orange-mottled, pebbly sandy silt grading downward into silty sand and then into silty sandy gravel. Nearer the fault, the clay content increases. On the east side of the fault, the basal unit (100?) is a massive orange mottled, light brown gravelly sandy clay. It looks somewhat different than the unit on the west side but is likely from the same source.

Overlying the unit 100 basal colluvium is a series of fluvial deposits consisting of gravel, sand, and silt. These are similar in appearance and provenance to those in trench T2, but individual units do not correlate between trenches (i.e. numbered units in T1 are not the same unit as identically numbered units in T2). On the east side of the fault, gravel (unit 70) overlies the basal clay-rich weathered colluvium (unit 100?). This is dry, loose, poorly sorted, pebble-cobble gravel, with maximum clast size of about 50 mm. Above this gravel, the stratigraphy consists of interfingering gravel and silty sand lenses. Unit 60 overlies unit 70 and is a finer-grained overbank deposit that consists of dry, hard, massive to lightly bedded, yellow-brown sandy silt to silty sand, with lenses of coarse sand and fine gravel. Unit 60 is present only on the east side of the fault. Above this finer unit is another gravel (unit 50). It is a dry, loose, massive to crudely bedded, pebble-cobble gravel, with a coarse sand to granule matrix; matrix content increases and clast size decreases at the east end of the trench.

On the west side of the fault, a coarse gravel (unit 70?) directly overlies unit 100. It is a dry, loose, poorly sorted sandy pebble-cobble gravel that varies between clast- and matrix-supported. Clasts reach 150 mm, and the matrix comprises sand to small pebbles. At the western end of the trench, a lens of dry, hard, loose, massive, silty coarse sand, with pockets of crudely bedded pebble gravel, separates the channel gravel from the underlying unit 100 colluvium. Although the clasts are larger, we consider that this gravel is probably approximately correlative with the unit 70 gravel east of the fault. This coarse gravel is directly overlain by more gravel (unit 50?), which we have differentiated based primarily on clast size. This upper gravel is a dry, loose, yellow-brown, poorly sorted, massive to crudely horizontally bedded, pebble gravel with some cobbles. It is largely matrix supported, with a coarse sand matrix. We tentatively correlate this with unit 50 on the east side of the fault, but the clast size is notably smaller.

The gravel on the west side of the fault has a well-developed channel morphology. It has cut into the underlying deposits and thickens abruptly near meter 4. This thick channel deposit has been cut by the fault at meter 6 and is not evident on the east side of the fault, although the unit 50 gravels are still present. Although the gravels may correlate across the fault, the channel on the east side has been faulted southeastwards and is no longer present at the trench location. The channel edge trends obliquely to the trench, and the channel appears to have flowed in a north-northeast direction.

Overlying the gravels is a highly bioturbated, yellow-brown, massive, pebbly sandy silt, with abundant



roots, charcoal, and krotovina (unit 40). This is topped by the modern "A" horizon topsoil.

Within the fault zone, units are hard to identify with certainty due to the shearing and disruption from faulting, but the general stratigraphy is apparent, with pockets of gravel and sandy silt tentatively associated with the major units defined outside the fault zone, except where very strongly sheared (e.g. within fault zone between meters 7 and 8). We have defined two other units within the fault zone. Unit F<sub>G</sub> is chaotic pebble-cobble gravel that we interpret as fissure fill formed in response to the penultimate event (discussed below) and subsequently faulted in the most recent event. R<sub>1906</sub> is a loose cobble gravel with sand-pebble matrix that we interpret as colluvium formed after the most recent (1906?) event from the raveling of exposed gravel from the free face formed in that event.

### Event Stratigraphy

The event stratigraphy in Trench 1 reveals a similar history to that in Trench 2, with evidence of two events since the deposition of the fluvial deposits overlying the basal weathered colluvium. The most recent event, which we assume was the 1906 earthquake, ruptured to near the current ground surface. Traces in the south wall extend to within about 20 cm of the top of unit 40 where they become indistinct within a large krotovina. In the north wall, the 1906 traces (red in Figure 8) extend well into unit 40 and are overlain by colluvial rubble raveled off the scarp free face.

The second event back ("Event G") occurred when only the lower part of the unit 40 sandy silt had been deposited and was at the ground surface. The fault traces associated with this event are shown in pink in Figure 8 and are located east of the 1906 traces, in a zone about a meter wide. Two traces at the eastern edge of this zone, at about meter 7.5, cut through the gravel units and into the base of the overlying overbank silts, bounding a sheared zone of mixed coarse and fine material. The westernmost of these two traces juxtaposes the sheared material against what is probably faulted unit 50? gravel. This contact is mapped with a dashed fault at the top, as the scarp face may be somewhat eroded, forming a free face-colluvial contact rather a fault contact; the relationship at the top of this fault is not certain. Thus the fault zone (colored orange in Figure 8) may include both material sheared into the zone during the event and some rubble eroded off the exposed scarp face that has modified the original fault contact. The western zone set of fault traces from the penultimate event occurs at about meter 6.5. Fault traces here extend into the bottom 10 cm or so of the unit 40 sandy silt. These traces are overlain by a line of gravel clasts (large pebble to small cobble size) within the silt unit that we interpret to be rubble raveled off the gravel exposed during the event. Event G also produced a fissure (F<sub>G</sub>) or colluvial rubble package filled with chaotic cobble gravel in a silty sand matrix. This fissure/rubble was subsequently faulted in the 1906 event and is overlain by the colluvial rubble (R<sub>1906</sub>) deposited after that event. The younger colluvium also contains cobble gravel but is distinguished from the older rubble by being looser and having a matrix of coarse sand to small pebbles as opposed to the finer silty sand matrix of the F<sub>G</sub> material.

There is no evidence in the trench for any other event since the start of deposition of the fluvial deposits that overlie the dark basal clay.

### **3.4 Age Constraints**

Age data from the CSS trenches are still preliminary. We obtained charcoal samples from throughout the section and submitted several for dating. The samples were analyzed by accelerator mass spectrometry (AMS) at Lawrence Livermore National Laboratory. The OxCal program (version 4.1.3) (Bronk-Ramsey 1995, 2001, 2009; Reimer et al. 2004a, 2004b) was used to determine the calibrated calendar age for each



radiocarbon sample. The samples were calibrated independently, not using a stratigraphic model. This model will be developed and the samples recalibrated accordingly in future.

Sample locations are shown on the logs, and the age data appear in Table 1. We dated a few samples from a variety of horizons but concentrated the dating on samples above and below the penultimate event horizon in the south wall of Trench 2 (Figure 9). All samples are detrital charcoal. In the following discussion, all dates are rounded to the nearest decade.

We dated one sample (T1N-5) from the basal weathered colluvial unit 100, which had a calibrated calendar date of 1260-1020 B.C. One other sample (T2S-2) was older (4330 BC - 3810 B.C.), but it was from a unit above unit 100 that contained numerous other samples of much younger age; we assume this has an inherited age and is much older than the age of the deposit.

In Trench T2, six samples were obtained from the unit 40 silt that overlies the colluvial wedge formed after Event G ("R" in Figures 9 and 7a). If our interpretation is correct, these should post-date Event G and the sample ages should be younger than those from pre-event deposits. Nine samples from the unit 40 silt below the colluvial wedge were dated; these should be older than Event G and older than the samples from above the colluvial wedge. By and large, these age relationships are borne out, with one notable exception.

The youngest post-event sample (T2S-8) has a calibrated calendar age of 1260-1380 AD. The other post-event sample ages are between 830 AD and 1280 AD, with the exception of T2S-4, which is significantly older, at 0-130 A.D. These data suggest that the post-event silt was deposited around 1300 AD, with some samples having some inherited age.

The samples from the silt below the colluvial wedge in the southeast wall of Trench T2 are older than the youngest post-event samples, with one exception. There is a group of three samples with calibrated ages around 1000 AD, three others with ages around 500 AD, and two much older samples, T2S-2 mentioned above and T2S-80 (780-540 BC). Three pre-event samples from Trench T1 also have ages around 1000 AD. These samples suggest that the post-event silt was deposited around 1000 AD, with some samples having inherited ages making them older than the deposit. Pre-Event G samples from Trench T1 have slightly younger ages, about 1100 AD. This would in turn suggest that Event G occurred between about 1000 AD and 1400 AD, given the uncertainties in the ages.

One pre-event sample is stratigraphically inconsistent with this interpretation. Sample T2S-77, from the unit 40 silt below the colluvial wedge, i.e. a pre-event sample, has a calibrated calendar date of 1420-1460 AD, the youngest sample date and younger than any of the samples obtained from the post-event silt. Two possibilities exist to explain this apparently anomalous age. The first possibility is that this sample age is correct and represents the maximum age of the pre-event deposit. This would imply that all other samples, both pre- and post-event, carry a significant inherited age and are much older than the deposits containing them. Furthermore, it implies that Event G post-dates 1420-1460 AD and is thus constrained to have occurred between 1420 and 1906 AD. The second possibility is that the other stratigraphically consistent samples flanking the Event G colluvial wedge are correct and there is a problem with sample T2S-77, such as having been obtained from an unrecognized krotovina. In that case, the interpretation noted in the preceding paragraph would still hold.

We intend to carry out further analysis of the samples and dates from the trenches. We have sent samples for detailed inspection in hopes of obtaining discrete identifiable plant remains, such as twigs and other



delicate organic materials, that are unlikely to have travelled far from the source or have a large inherited age. If we isolate and date these, we hope to minimize the likelihood of overestimating the age of the deposits, as can commonly happen with use of detrital charcoal. In addition, we will develop a stratigraphic model for the trenches, with the existing and new dates, and use OxCal analysis to a probability density function around the preferred event age for Event G. Pending this analysis, our preferred working interpretation is that there is a problem with T2S-77 and the other samples best reflect the ages of the deposits.

We collected bulk samples from several locations within the trenches to sample for pollen. The presence of non-native *Erodium cicutarium* pollen in sediments has been used to date the deposits as being historical in age. *Erodium* was introduced and became prevalent throughout the San Francisco Bay Area shortly following the arrival of the Spanish in 1772 (HPEG, 1999). The absence of *Erodium* has also been used to indicate a pre-1800 age of deposits. In the case of our samples, no *Erodium* pollen was found. However, no other type of pollen was found in the samples either, so the pollen results are inconclusive.



#### 4.0 DISCUSSION

The CSS trenches exposed a suite of fluvial deposits that are younger than the 1260-1020 BC weathered colluvium (unit 100) at the base of both trenches. Samples (e.g. T2N-1 and T1S-1) from the channel gravels that overlie the older clay-rich unit in both trenches had calibrated ages of about 1000 to 1100 AD. The bulk of the overlying deposits appear, based on the sample ages (excluding T2S-77), to have been deposited within a few hundred years, as the sample ages are all older than 1380 AD (Sample T2S-8). The age of the uppermost half-meter or so of deposits is unknown because the extensive bioturbation precluded sampling within this range. Only two faulting events have been identified in the trench as having occurred within this part of the exposure. The most recent earthquake recorded in the section we assume is the 1906 earthquake. The older event occurred between about 1000 and 600 years ago, if the ages of samples other than TS2-77 approximately reflect the ages of the deposits, or between 1420 and 1906 AD, if all other samples have a large inherited age and sample TS2-77 more closely reflects the age of the deposits.

Assuming the former interpretation is correct, the data from these trenches suggest that the penultimate event on this part of the San Andreas fault occurred many hundreds of years before the 1906 event. These results are similar to those found at the Crystal Springs site north of the reservoir, where Prentice et al. (2008) found only one pre-1906 event dated about 1000 years ago, but differ somewhat from results from Portola Valley, where Baldwin and Prentice (2008) report 3-4 events in the past 1000 years, and perhaps from Filoli, where relatively inconclusive data have been interpreted to suggest a pre-1906 event occurred since ca. 330 BP (Hall et al., 1999). They also differ markedly from the paleoseismic record at the Mill Canyon-Arano Flat site on the Santa Cruz Mountains segment of the San Andreas fault, where Fumal et al. (2003) find evidence of nine events in about 1000 years. At the Hazel Dell site, about 10 km northeast of Arano Flat, three to four events (including 1906) have occurred since 674 AD, noticeably fewer than at Arano Flat but still more than observed at CSS (Figure 2; Streig and Dawson, 2009).

As at the Crystal Springs and Portola Valley sites, there is as yet no evidence of an event in 1838 at CSS. To date, the only geologic evidence that has been found to support the 1838 event on the San Andreas fault is an offset 330 BP-aged channel at Filoli interpreted by Hall et al. (1999) as possibly offset during the 1838 earthquake. Yet, there is just one possible interpretation of the data. Zachariassen et al. (2010) reanalyzed the Hall et al. (1999) offset data and concluded that, whereas their channel reconstruction was a plausible one, equally plausible reconstructions would allow greater or lesser amounts of offset, beyond their stated uncertainties. Based on that reassessment, Zachariassen et al. (2010) concluded that the data can be interpreted to indicate that the older channel was offset by only a single event, 1906. Thus, it is possible that there is only one recent earthquake (1906) at Filoli, with the penultimate event being perhaps much older than 1838. If our preferred interpretation of the sample data is wrong, such that all samples except perhaps TS2-77 are much older than their deposits and the penultimate event occurred after 1417 AD, it could conceivably be the 1838 event. However, we think this unlikely, especially given the amount of deposition of fine-grained overbank deposits that would have to have occurred between 1838 and 1906. Certainly there is no explicit support for the event.

The dating results are still preliminary and further work may alter the interpretation. To date, however, the CSS trench data suggest only two events have occurred at the site in about 1000 years: one in 1906 and a second event about 600-1000 years ago. This is fewer than have been found at Portola Valley and Hazel Dell and far fewer than have been found at Arano Flat to the south. One possible interpretation is that there are missing events at CSS. The fault may have ruptured here but left no signature that we have yet identified, or slip may have occurred on another trace than the 1906 trace; a latest-Quaternary trace



that did not rupture in 1906 has been mapped to the west of the site (Figure 2; USGS/CGS, 2006). The similarity to results to the north at the Crystal Springs site, however, along with stratigraphic and faulting relationships that argue against additional events in the CSS trenches, preclude an easy dismissal of the event history obtained from the CSS trenches and suggest the possibility of long recurrence intervals, or at least a long interval between 1906 and the penultimate event, along this part of the Peninsula section. If this is true, it suggests that models in which the entire northern San Andreas ruptures together in 1906-like events may not be the best or most representative of the fault rupture behavior. Furthermore, the segmentation model that has formed the basis of the last several iterations of seismic hazard maps in general may be incorrect. Paleoseismic data from sites to the south (Arano Flat-Mill Canyon, Hazel Dell, and Portola Valley) suggest increasing average recurrence interval northward, with Arano Flat having a much shorter interval than the other two sites, which are in turn shorter than the last interval at CSS. It may be that the model of segmentation, in which the fault is divided into a small number of long-lived segments that rupture characteristically, either with other segments or alone, should be replaced with a model that reflects greater spatial and temporal variability in rupture patterns.

The CSS paleoseismic site is promising, yielding some of the best stratigraphy of any site on the Peninsula section of the San Andreas. The potential for acquiring further information from this site is high. In particular, the large channel in Trench T1 that is evident on the west side of the fault and has been offset to the southeast on the east side promises to be a good candidate for determining displacement. The offset in 1906 at locations north and south of the CSS site was about 8-8.5 ft, or about 2.5 m. The slip rate over the last 2000 years at Filoli is  $17 \pm 4$  mm/yr. Over 1000 years, at that slip rate, about 17 m of slip should have accumulated on the fault. If only 2 events have occurred within 1000 years, and the last event had only 2-3 m of slip, it suggests either that a slip deficit has accumulated on the fault, the slip rate is irregular, or that some fraction of the total slip rate is occurring off the fault in this area. The eastern part of the channel, which is about 1000 years old, should be present east of the fault, southeast of and within 20 meters or so of Trench T1. Excavating fault parallel trenches between Trenches T1 and T2 should expose the offset channel and provide information about total offset. If the total offset is closer to 17 m, it suggests that either events are missing in Trenches T1 and T2, since it is unlikely that the penultimate event would have had a 14- m rupture prior to the 3-m 1906 rupture, or that the radiocarbon dates are all much older than the actual date of deposition of the fluvial deposits. If the total offset is closer to 6 m, it suggests the event history as presented here is correct, only two events have occurred in 1000 years, and there is a slip deficit on the fault that should be investigated further.



## 5.0 CONCLUSIONS

The Peninsula section of the San Andreas fault ruptured in the 1906 San Francisco earthquake, but it is unclear when the penultimate event occurred. The 1838 earthquake has been proposed as a San Andreas event, but no direct paleoseismic evidence of that event has been found to date. Hall et al. (1999) argued that an event near that time occurred at the Filoli site, but their data allow the interpretation that no recent (ca. 19th c.) events occurred prior to 1906. The Crystal Springs trenches of Prentice et al. (2008) showed evidence of the most recent event (1906) and one older event dated around 1000 years ago. In this study, trenches at the Crystal Springs South paleoseismic site also suggest that the most recent event prior to 1906 to have ruptured the ground surface occurred about the same time. Additional sampling and dating is required to clarify the ages with certainty, but initial dating results suggest the penultimate event occurred about 600-1000 years ago (between ca. 1040-1385 AD). There is no evidence of an 1838 event nor, in our preferred interpretation of the dating results, of any other event between 1906 and 1385 AD. The absence of evidence for an 1838 event is consistent with recent results from Crystal Springs, Portola Valley, and Hazel Dell paleoseismic sites.

Results from the CSS trenches indicate that events on the Peninsula section, or at least this part of the Peninsula section, may be less frequent than has been assumed. Given the preferred slip rate here of  $17 \pm 4$  mm/yr, a long interval between the last two events may indicate a large accrued slip deficit on the fault, temporally or spatially variable slip rate, or off-fault deformation. Alternatively, there may be missing events in the trench record at CSS. Further studies at the site, especially investigating an offset channel exposed in Trench 1, may help clarify this issue.



## **6.0 ACKNOWLEDGMENTS**

Appreciation goes to the City and County of San Francisco and the Natural Resources and Lands Management Division of the San Francisco Public Utilities Commission for giving permission to work at the site in the watershed and providing biological and cultural monitoring services for the excavation. Keith Dick of Keith's Excavating dug and backfilled the trenches for us. The field and office assistance provided by Robert Sickler, Anne Sanquini, Keith Knudsen and Jennifer Mendonça is greatly appreciated. Susan Olig provided technical review comments that improved the report.





## 7.0 REFERENCES

- Bakun, W.H., 1999, Seismic activity of the San Francisco Bay region, *Bulletin of the Seismological Society of America*; June 1999; v. 89; no. 3; p. 764-784.
- Baldwin, J. and Prentice, C., 2008, Earthquake records of the Peninsula segment of the San Andreas fault, Portola Valley, California: Collaborative research with William Lettis & Associates, inc. and U.S. Geological Survey, Final Technical Report, U. S. Geological Survey National Earthquake Hazards Reduction Program Award Number 05HQGR0073.
- Baldwin, J., Prentice, C., Wetenkamp, J., and Sundermann, S., 2006, Preliminary Earthquake Record of the Peninsula Section of the San Andreas fault, Portola Valley, California, *Seismological Research Letters* Volume 77, Number 2, p. 248.
- Bronk Ramsey, C., 2009, Bayesian analysis of radiocarbon dates, *Radiocarbon*, 51(1), p. 337-360.
- Fumal, T.E. Heingartner, G.F. Samrad, L., Dawson, T.E., Hamilton, J.C., and Baldwin, J.N., 2003, Photomosaics and Logs of Trenches on the San Andreas Fault at Arano Flat near Watsonville, California: U.S. Geological Survey Open-File Report 03-450, Version 1.0.
- Hall, N.T., Wright, R.H., and, C.S. Prentice, 2001, Studies along the peninsula segment of the San Andreas fault, San Mateo and Santa Clara Counties, California *in* Ferriz, H., and Anderson, R., eds., *Engineering Geology Practice in Northern California: California Division of Mines and Geology, Bulletin 210, Special Publication 12*, p. 193 - 210.
- Hall, N.T., Wright, R.H., and Clahan, K.B., 1999, Paleoseismic studies of the San Francisco peninsula segment of the San Andreas fault zone near Woodside, California: *Journal of Geophysical Research*, v. 104, no. B10, p. 23,215-23,236.
- Hayward fault Paleoeearthquake Group (HPEG) (J. J. Lienkaemper, D.P. Schwartz, K.I. Kelson, W.R. Lettis, G.D. Simpson, J.R. Southon, J.A. Wanket, P.L. Williams), 1999, Timing of Paleoeearthquakes on the Northern Hayward Fault — Preliminary Evidence in El Cerrito, California, U. S. Geological Survey Open-File Report 99-318
- Knudsen, K.L., Witter, R.C., Garrison-Laney, C.E., Baldwin, J.N., and Carver, G.A., 2002, Past earthquake-induced rapid subsidence along the northern San Andreas fault: A paleoseismological method for investigating strike-slip faults: *Bulletin of the Seismological Society of America*, v. 92, no. 7, p. 2612-2636.
- Lawson, A.C., 1908, The earthquake of 1868; *in* A.C. Lawson, ed., the California earthquake of April 18, 1906: Report of the State Earthquake Investigation Commission (vol. 1): Carnegie Institute of Washington Publication 87.
- Prentice, C. and Moreno, X., 2007, Paleoseismic site on the Peninsula San Andreas fault near Crystal Springs Reservoir: Preliminary results, *Seismological Research Letters* Volume 78, No. 2, p.315.
- Prentice, C.S., Sickler, R.S.; Hecker, S.; Schwartz, D.P., Brown, J., 2008, Preliminary results from a new paleoseismic site on the San Andreas fault near Crystal Springs Reservoir, San Francisco peninsula, California, , *Seismological Research Letters* Volume 79, No. 2, p.360.
- Reimer, P. J., Baillie, M. G. L., Bard, E., Bayliss, A., Beck, J. W., Blackwell, P. G., Bronk Ramsey, C.,



- Buck, C. E., Burr, G. S., Edwards, R. L., Friedrich, M., Grootes, P. M., Guilderson, T. P., Hajdas, I., Heaton, T. J., Hogg, A. G., Hughen, K. A., Kaiser, K. F., Kromer, B., McCormac, F. G., Manning, S. W., Reimer, R. W., Richards, D. A., Southon, J. R., Talamo, S., Turney, C. S. M., van der Plicht, J., & Weyhenmeyer, C. E., 2009, IntCal09 and Marine09 radiocarbon age calibration curves, 0-50,000 years cal BP, *Radiocarbon*, 51(4), p. 1111-1150.
- Schwartz, D.P., Pantosti, D., Okumura, K., Powers, T.J., and Hamilton, J., 1998, Paleoseismic investigations in the Santa Cruz mountains, California: Implications for recurrence of large-magnitude earthquakes on the San Andreas fault: *Journal of Geophysical Research*, v. 103, no. B8, p. 17,985-18001.
- Streig, A.R. and Dawson, T.M., 2009, Paleoseismic Record Of Earthquakes on The Santa Cruz Mountains Segment of The San Andreas Fault - Testing The Influence of The Northern Transition Zone Using Earthquake Chronologies and Implications for Seismic Hazards on The San Andreas Fault: Collaborative Research with William Lettis and Associates Inc. and the California Geological Survey, Final Technical Report for US Geological Survey National Earthquake Hazard Reduction Program, Award Numbers 08-HQ-GR-0071 and 08-HQ-GR-0072, [earthquake.usgs.gov/research/external/reports/08HQGR0071.pdf](http://earthquake.usgs.gov/research/external/reports/08HQGR0071.pdf).
- Topozada, T.R., and Borchardt, G., 1998, Re-evaluation of the 1836 "Hayward Fault" earthquake and the 1838 San Andreas Fault earthquake: *Seismological Society of America Bulletin*, v. 88, p. 140-159.
- U.S. Geological Survey and California Geological Survey (USGS/CGS), 2006, Quaternary fault and fold database for the United States, accessed June and July 2011, from USGS web site: <http://earthquakes.usgs.gov/regional/qfaults/>.
- 2007 Working Group on California Earthquake Probabilities (WGCEP), 2008, The Uniform California Earthquake Rupture Forecast, Version 2 (UCERF 2), USGS Open File Report 2007-1437, CGS Special Report 203, SCEC Contribution #1138, Version 1.0
- Working Group on California Earthquake Probabilities ((WGCEP), 2003, Earthquake Probabilities in the San Francisco Bay Region: 2002–2031, USGS Open-File Report 03-214.
- Working Group on California Earthquake Probabilities (WGCEP), 1988, Probabilities of large earthquakes occurring in California on the San Andreas fault, U.S. Geological Survey Open-File Report, p. 62.
- Working Group on California Earthquake Probabilities (WGCEP), 1990, Probabilities of large earthquakes in the San Francisco Bay Region, California, U.S. Geological Survey Circular, p. 51.
- Working Group on Northern California Earthquake Potential (WGNCEP), 1996, Database of potential sources for earthquakes larger than magnitude 6 in northern California: U. S. Geological Survey Open-File Report 96-705.
- Zachariassen, J. A.; Prentice, C. S.; Kozaci, O.; Sickler, R. R.; Baldwin, J. N.; Sanquini, A.; Knudsen, K. L., 2010, Paleoseismic Study on the Peninsula Section of the San Andreas Fault South of Crystal Springs Reservoir, San Mateo County, California, American Geophysical Union, Fall Meeting 2010, abstract #S21C-2048.
- Zhang, H., Niemi, T., and Fumal T., 2006, A 3000-year record of earthquakes on the northern San



**FUGRO WILLIAM LETTIS & ASSOCIATES, INC.**

---

Andreas fault at the Vedanta marsh site, Olema, California: Seismological Research Letters, v. 77, p. 176.

**Table 1. Radiocarbon Data from Crystal Springs South Trenches 1 and 2, August 2010**

CAMS # <sup>1</sup>	Sample Name <sup>2</sup>	$\delta^{13}\text{C}$ <sup>3</sup>	Fraction Modern	Uncertainty ±	$\text{D}^{14}\text{C}$	Uncertainty ±	$^{14}\text{C}$ age (BP) <sup>4</sup>	Uncertainty ±	Calibrated Age (Calendar Date) <sup>5</sup>	Notes
149895	T2S-8	-25	0.9163	0.0027	-83.7	2.7	700	25	1264-1385 AD	Post-Event G
149915	T2S-3	-25	0.9110	0.0027	-89.0	2.7	750	25	1224-1285 AD	Post-Event G
149044	T1N-4	-23.12	0.9015	0.0024	-98.5	2.4	835	25	1163-1259 AD	Unit 40 silt; Post-Event G?
149894	T2S-6	-25	0.8937	0.0026	-106.3	2.6	905	25	1030-1208 AD	Post-Event G
149893	T2S-5	-25	0.8877	0.0020	-112.3	2.0	955	20	1022-1155 AD	Post-Event G
149896	T2S-58	-25	0.8695	0.0026	-130.5	2.6	1125	25	833-989 AD	Post-Event G
149916	T2S-4	-25	0.7870	0.0026	-213.0	2.6	1925	30	2-134 AD	Post-Event G
149910	T2S-77	-25	0.9449	0.0029	-55.1	2.9	455	25	1417-1464 AD	Pre-Event G
149043	T1N-2	-24.03	0.8943	0.0029	-105.7	2.9	900	30	1040-1211 AD	Pre-Event G silt
149047	T1S-2	-23.50	0.8875	0.0027	-112.5	2.7	960	25	1021-1155 AD	Pre-Event G gravel
149908	T2S-75	-25	0.8849	0.0026	-115.1	2.6	980	25	995-1154 AD	Pre-Event G
149906	T2S-51	-25	0.8827	0.0026	-117.3	2.6	1000	25	987-1150 AD	Pre-Event G
149907	T2S-52	-25	0.8830	0.0026	-117.0	2.6	1000	25	987-1150 AD	Pre-Event G
149048	T2N-1	-25.27	0.8792	0.0027	-120.8	2.7	1035	25	903-1030 AD	Pre-Event G gravel
149046	T1N-6	-23.24	0.8766	0.0027	-123.4	2.7	1060	25	898-1023 AD	Pre-Event G gravel
149912	T2S-79	-25	0.8290	0.0025	-171.0	2.5	1505	25	441-622 AD	Pre-Event G
149905	T2S-50	-25	0.8205	0.0024	-179.5	2.4	1590	25	416-540 AD	Pre-Event G
149909	T2S-76	-25	0.8148	0.0025	-185.2	2.5	1645	25	335-532 AD	Pre-Event G
149913	T2S-80	-25	0.7323	0.0022	-267.7	2.2	2505	25	781-538 BC	Pre-Event G
149049	T2S-2	-25	0.5205	0.0052	-479.5	5.2	5250	90	4328-3813 BC	Pre-Event G
149045	T1N-5	-25	0.6944	0.0026	-305.6	2.6	2930	30	1259-1024 BC	Unit 100 colluvium

Radiocarbon concentration is given as fraction Modern,  $\text{D}^{14}\text{C}$ , and conventional radiocarbon age. Sample preparation backgrounds have been subtracted, based on measurements of samples of 14C-free coal. Backgrounds were scaled relative to sample size.

<sup>1</sup> Laboratory sample number. Center for Accelerator Mass Spectrometry (CAMS), Lawrence Livermore National Laboratory.

<sup>2</sup> Field trench sample number. Sample numbers include trench identification (T1 or T2), wall from which sample was obtained (S or N), and sample number. Logs show just the sample numbers.

<sup>3</sup>  $\delta^{13}\text{C}$  values are the assumed values according to Stuiver and Polach (Radiocarbon, v. 19, p.355, 1977) when given without decimal places. Values measured for the material itself are given with a single decimal place.

<sup>4</sup> The quoted age is in radiocarbon years using the Libby half life of 5568 years and following the conventions of Stuiver and Polach (1977). Uncertainties are 1 standard deviation. Years BP = years before 1950.

<sup>5</sup> Calibrated calendar age ranges at 95.4% confidence level, using Oxcal v4.1.3 (Bronk Ramsey, 2009) and calibration curve of Reimer et al., 2009). Simple calibration, without use of a stratigraphic model.

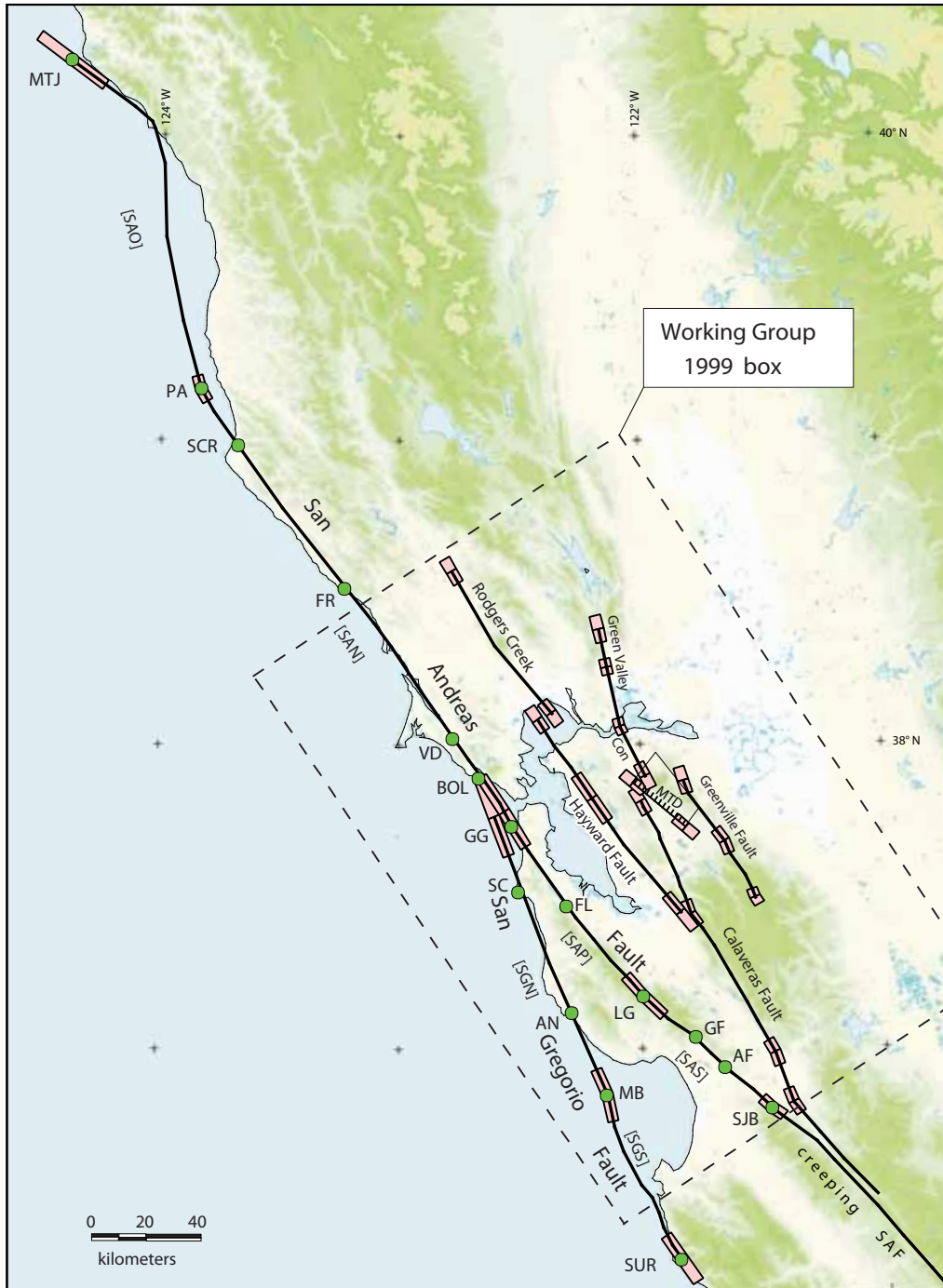


Figure 1. Map of the northern San Andreas fault system, with segmentation (segment boundaries shown with pink boxes). From WGCEP (2003). Segments of San Andreas fault (SAF): SAO - Offshore; SAN - North Coast; SAP - Peninsula; SAS - Santa Cruz Mountains. Sites along SAF (dots): MTJ - Mendocino triple junction; PA - Pt. Arena; SCR - Scaramella Ranch; FR - Fort Ross; VD - Vedanta; BOL - Bolinas Lagoon; FL - Filoli; LG - Los Gatos bend in SAF; GF - Grizzly Flat; AR - Arano Flat; SJB - San Juan Bautista. Other abbreviations: SGN - San Gregorio North segment; SGS - San Gregorio South segment; GG - Golden Gate; SC - Seal Cove; AN - Ano Nuevo; MB - Monterey bend in San Gregorio fault; SUR - Point Sur; MTD - Mt. Diablo Thrust; Con - Concord fault.

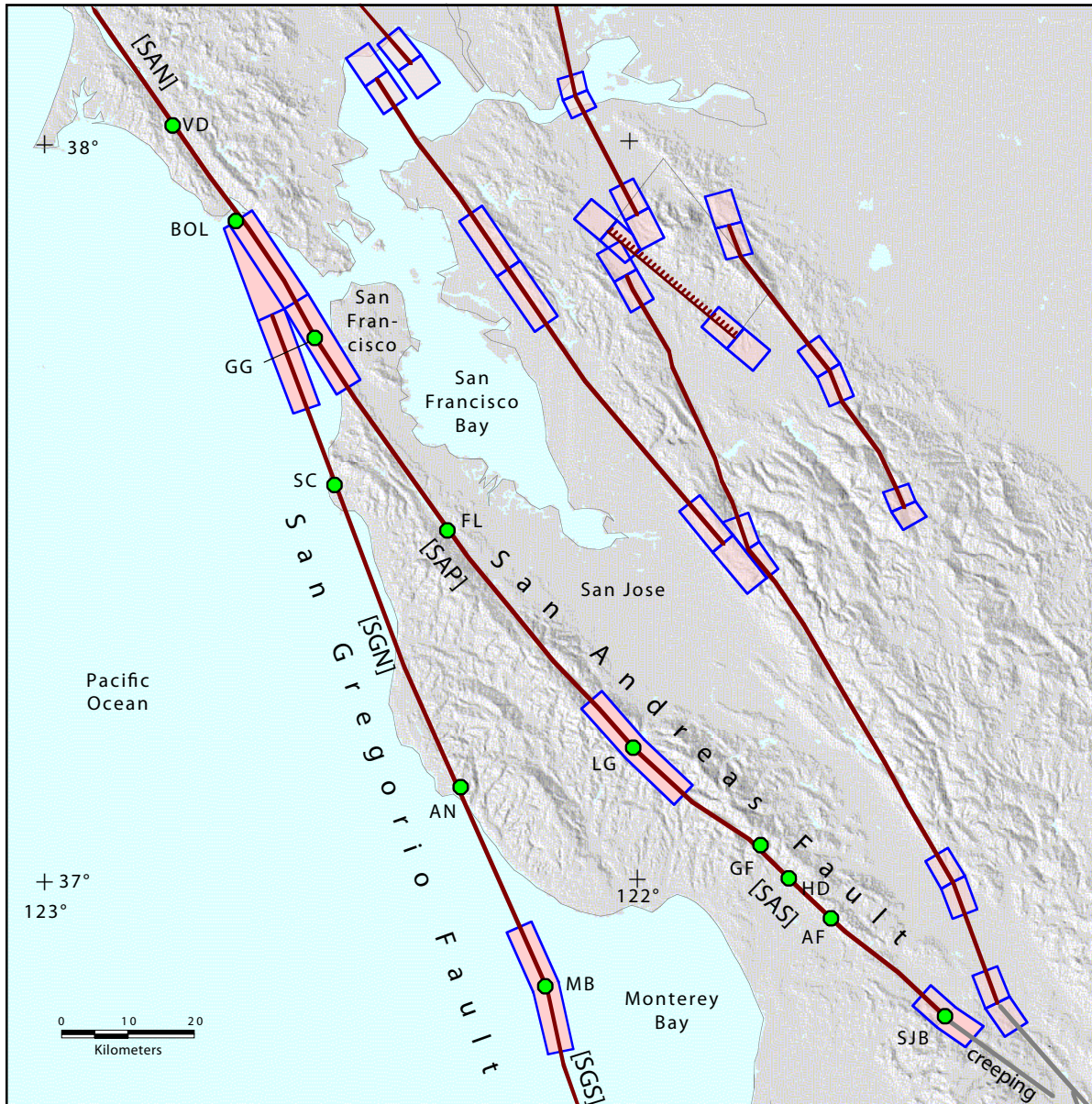


Figure 2. WGCEP (2003) map of the Peninsula (SAP) and adjacent segments (modified to add Hazel Dell paleoseismic site). Pink boxes mark segment boundaries. Green dots identify specific locations, including paleoseismic sites Filoli (FL), Arano Flat (AF), Grizzly Flat (GF), Hazel Dell (HD). CSS is Crystal Springs South site. Other abbreviations are as in Figure 1.



Figure 3. San Andreas fault Peninsula segment near Woodside, CA. Fault mapping from USGS Quaternary fault and fold database (<http://earthquake.usgs.gov/regional/qfaults/>). Colored dots show existing paleoseismic sites, including this study (blue dot).

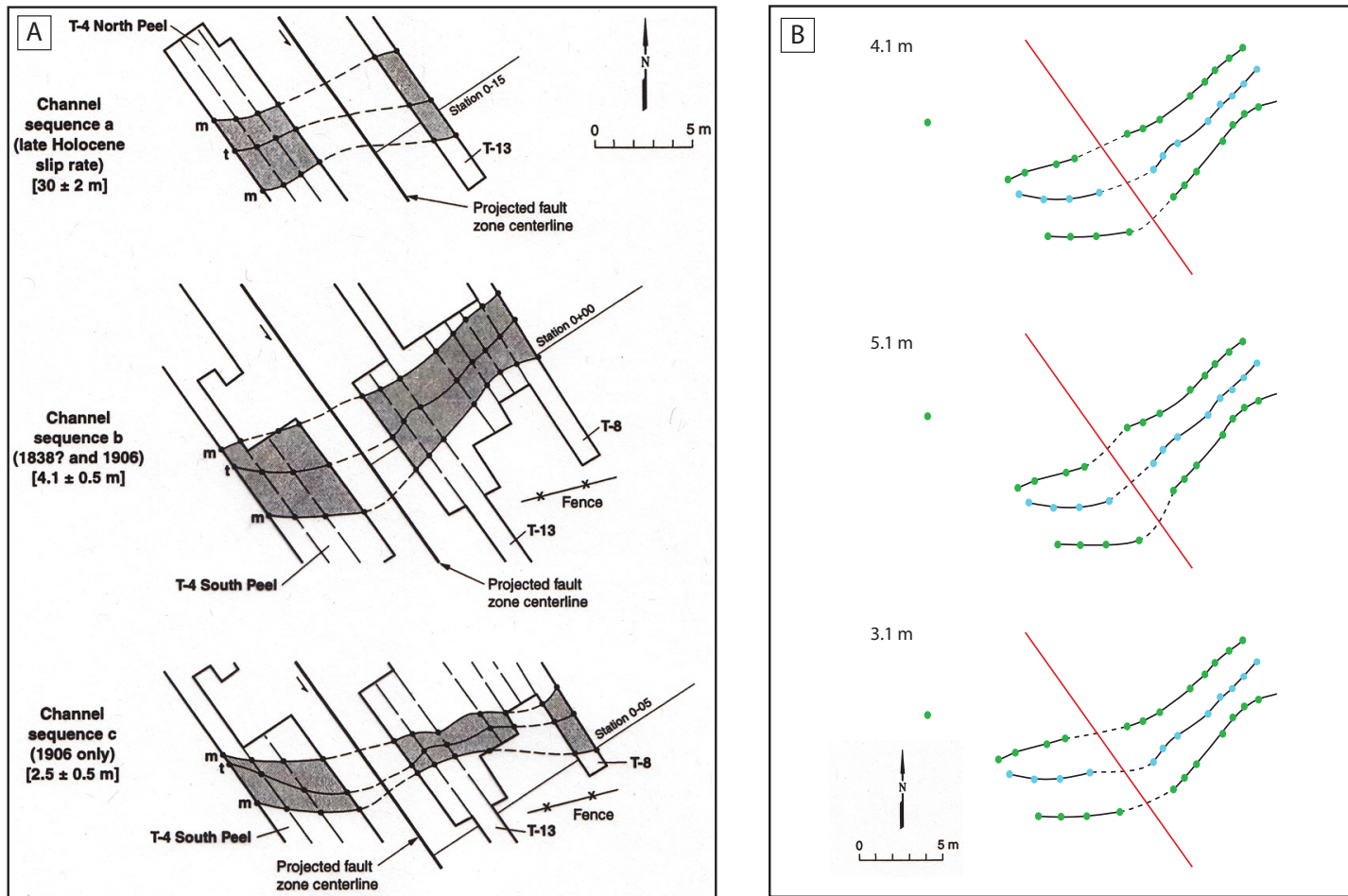


Figure 4. Alternative reconstructions of channel offset from the Filoli paleoseismic site. A. Figure 8, from Hall et al., 1999, showing their reconstructions of offset channels, which they conclude indicates the occurrence of a pre-1906 earthquake, with 1.6 m of offset. These reconstructions are based on projecting thalweg locations and channel edges across the fault. These reconstructions are valid interpretations of the data, but are not unique. B. Two alternate reconstructions of the Hall et al. (1999) data that provide geologically reasonable original configurations for channel b. The data permit that the two channels are offset the same amount, or that channel b is offset twice as much as c. Blue and green dots show exposures of thalweg and +0.5m contour of channel edge, respectively. Solid red line is approximate centerline of fault zone. Dashed lines are possible projections of channel features across fault zone.

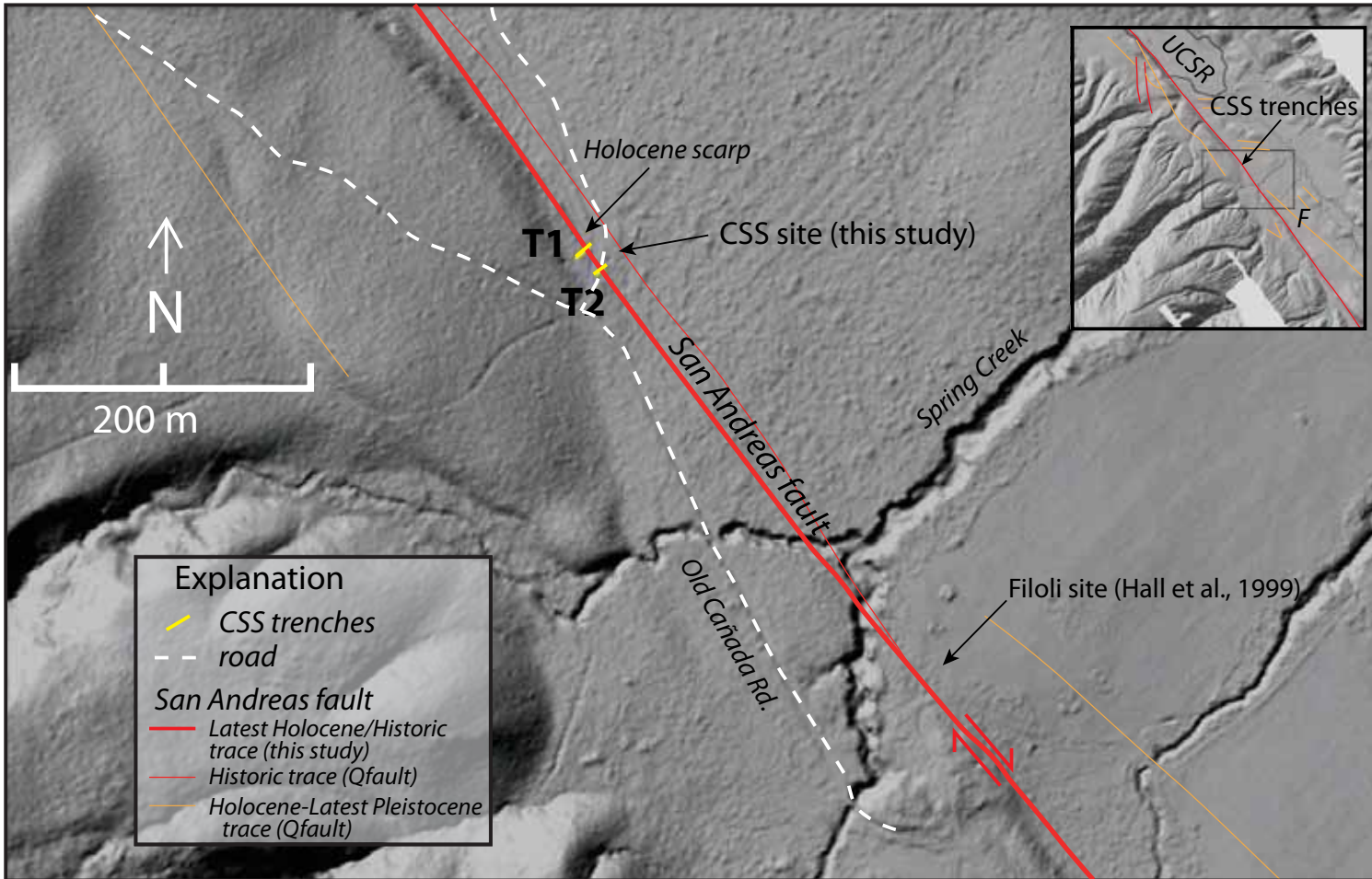
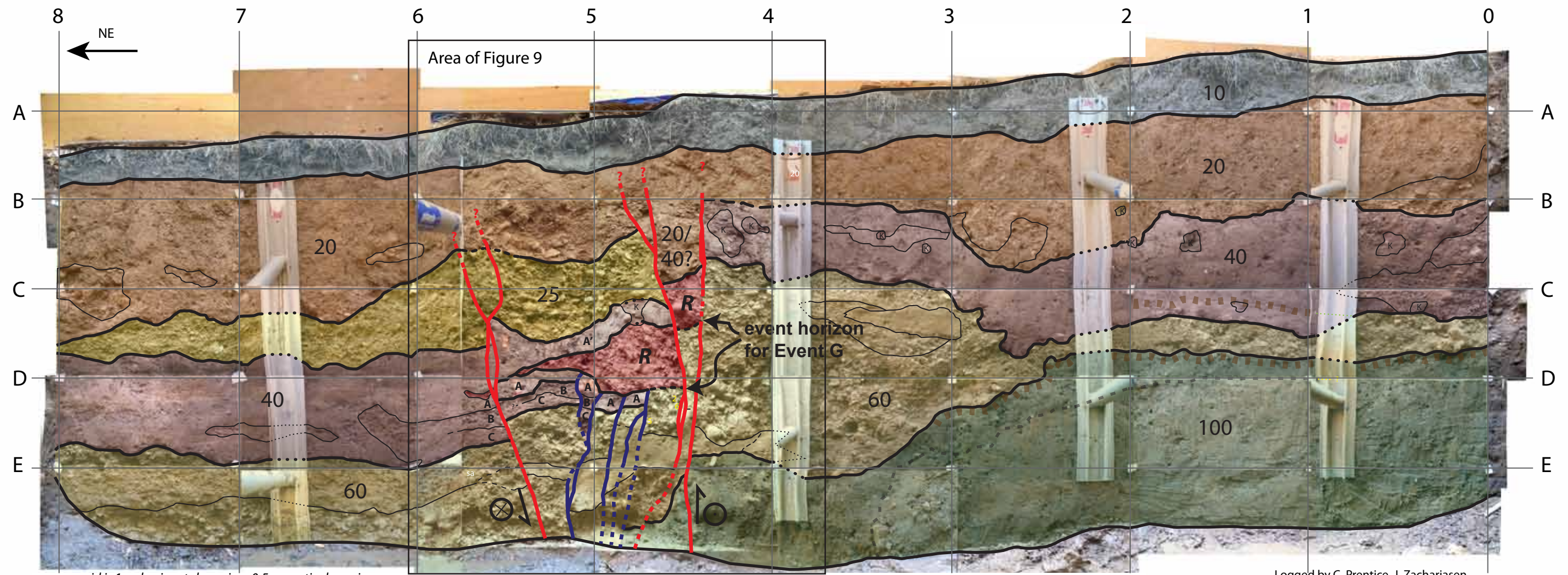


Figure 5. Bare earth DEM obtained from National Science Foundation Geoeathscope LiDAR data of Crystal Springs South (CSS) site. Faults in light line weight are from USGS Quaternary fault database (“Qfault”) map (USGS/CGS, 2006; compiled at 1:750,000). Modified fault mapping between CSS site and Filoli site (done for this study) is shown in heavy line weight. Trenches excavated in 2010 (in yellow) cross the fault where a small latest Holocene scarp is present outboard of the higher, eroded scarp. CSS trench site is protected from high stream flows by the fault scarp, which is eroded back from the fault and buried by fan deposits. Inset shows location of site relative to Upper Crystal Springs reservoir (UCSR) and Filoli Estates (F); faults from USGS/CGS (2006).



Figure 6. Photograph of trench site. View is to the south. Red line marks approximate location of fault.



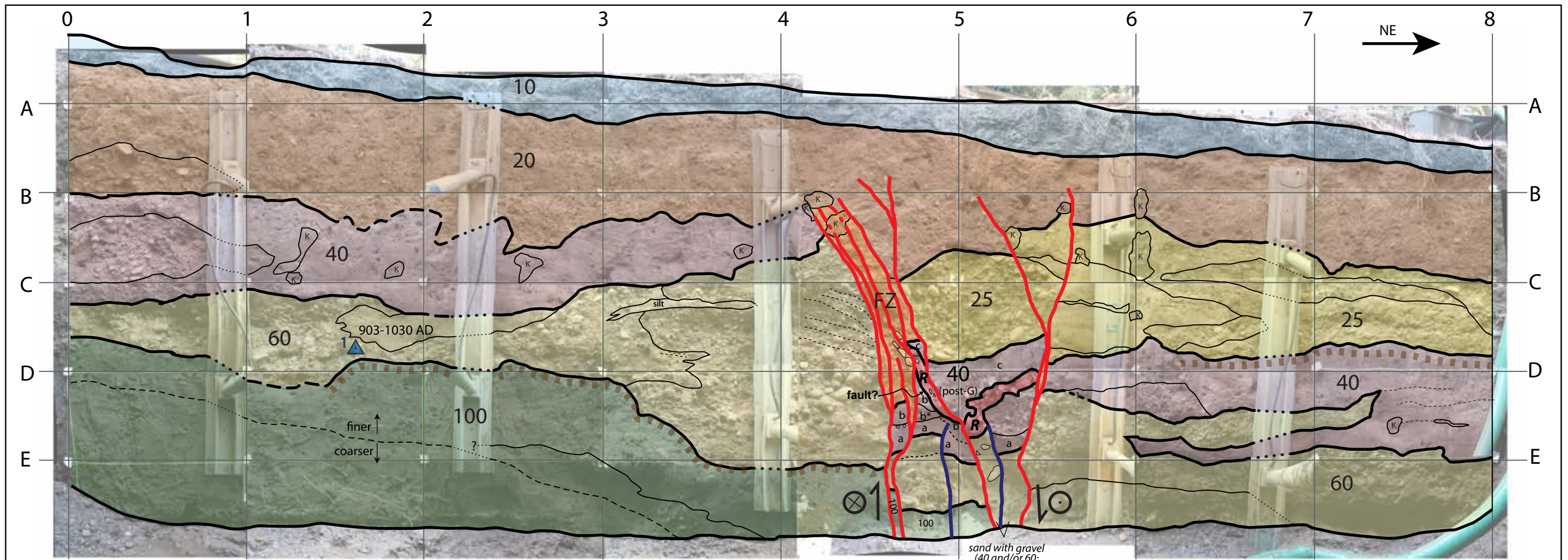
grid is 1-m horizontal spacing, 0.5-m vertical spacing

Logged by C. Prentice, J. Zachariassen  
August 2010

### EXPLANATION

<p><b>10</b> Topsoil (A horizon)</p> <p><b>20</b> Massive sandy pebbly silt with abundant bioturbation</p> <p><b>25</b> Well-rounded pebble-cobble gravel in coarse sand matrix; present only on downthrown side</p> <p><b>R</b> Colluvial wedge rubble, derived from unit 60; chaotic pebble-cobble gravel</p>	<p><b>40</b> Brown, massive, silty fine sand to sandy silt, with scattered pebbles and abundant charcoal; hatchures mark paleosol. Fault zone sub-units: A (pre-Event G) - silty sand; A' (Post-Event G) - very fine sandy silt; B - sandy granule gravel; C - sand</p> <p><b>60</b> Channel complex; well-rounded, clast-supported pebble-cobble gravel, with lenses of finer sand and silt</p> <p><b>100</b> Grey, mottled sandy silty clay to clayey silty sand with scattered pebbles and sparse large clasts; clasts deeply weathered; hatchures mark change in color from dark grey above to orange mottled below</p>	<p> Most recent event (1906?) fault traces</p> <p> Penultimate event ("event G") fault traces</p> <p> Color change in unit 100: medium grey above, light grey with orange mottling below</p> <p> Paleosol</p> <p>"K" indicates krotovina Light line weight contacts mark lenses of different material within numbered unit</p>
---	---	--

Figure 7a. Log of southeast wall of Trench T2. Trench exposed late Holocene coarse-grained channel and fine-grained overbank material interbedded with scarp-derived colluvium. Units in Trench T1 do not necessarily correlate with units with same numbers in Trench T2. Stratigraphic and structural relations provide evidence for two ground rupturing events: (1) the MRE (presumably 1906) is expressed by fault strands (shown in red) approaching the ground surface and terminating in a heavily bioturbated zone that is overlain by recent sediment; (2) The penultimate event (Event G) represents the displacement of the lower part of unit 40 (sub-unit "A" constituted the ground surface in Event G) across several fault strands (shown in purple). Event G exposed units 40 and 60, generating cobbly colluvium (R) derived from unit 60 that was deposited onto the paleo-surface "A". Deposition of unit 40 (A') overbank silts continued after Event G. Radiocarbon analysis of detrital charcoal from pre- and post-event deposits (A and A', respectively) indicate that Event G occurred about 600-1000 years ago.



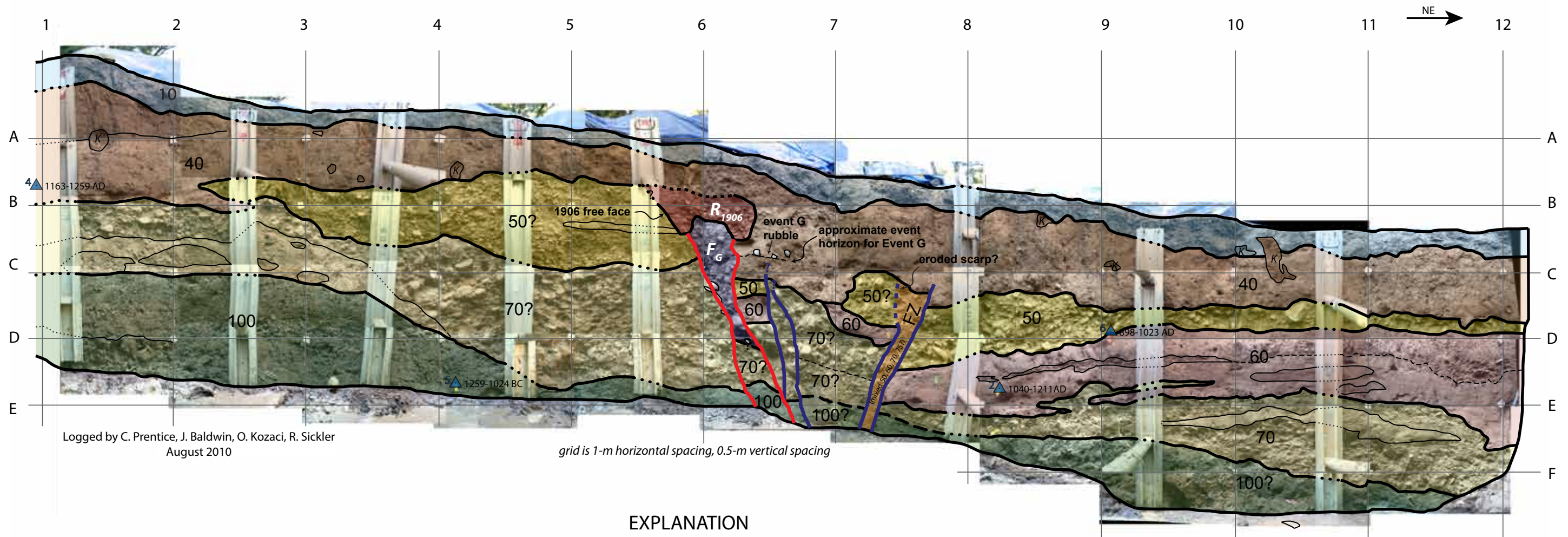
grid is 1-m horizontal spacing, 0.5-m vertical spacing

Logged by C. Prentice, J. Zachariasen, J. Baldwin, O. Kozaci  
August 2010

### EXPLANATION

- |   |  |   |
|---|--|---|
| <p><b>10</b> Topsoil (A horizon)</p> <p><b>20</b> Massive sandy pebbly silt with abundant bioturbation</p> <p><b>25</b> Well-rounded pebble-cobble gravel in coarse sand matrix; present only on downthrown side</p> <p><b>40</b> Brown, massive, silty fine sand to sandy silt, with scattered pebbles and abundant charcoal; hatchures mark paleosol.<br/>Fault zone sub-units: a) clean sand within channel complex; b) silty sand with pebbles (b* more gravel, pebble gravel in m-f sandy matrix), pre-G; c) post-event G sandy silt</p> | <p><b>R</b> Colluvial wedge rubble, derived from unit 60; chaotic pebble-cobble gravel; in westernmost sliver of R, f-c pebble gravel is mostly f-c pebbles in a silty matrix (possibly including 40c, post-G silt), sheared in 1906 fault zone</p> <p><b>FZ</b> Sheared gravel, silt and sand in fault zone</p> <p><b>60</b> Channel complex; well-rounded, clast-supported pebble-cobble gravel, with lenses of finer sand and silt</p> <p><b>100</b> Grey, mottled sandy silty clay to clayey silty sand with scattered pebbles and sparse large clasts; clasts deeply weathered; hatchures mark change in color from dark grey above to orange mottled below</p> | <p><b>1</b> <sup>903-1030 AD</sup> Radiocarbon sample location with calibrated age.</p> <p>Most recent event (1906?) fault traces</p> <p>Penultimate event ("event G") fault traces</p> <p>Bedding</p> <p>Paleosol</p> <p>"K" indicates krotovina<br/>Light line weight contacts mark lenses of different material within numbered unit</p> |
|---|--|---|

Figure 7b. Log of northwest wall of Trench T2.



### EXPLANATION

- |  |   |   |
|--|---|---|
| <p><b>10</b> Topsoil (A horizon)</p> <p><b>40</b> Massive pebbly sandy silt with abundant bioturbation</p> <p><b><math>R_{1906}</math></b> Post-1906 colluvium; loose cobble gravel with coarse sand and small pebble matrix</p> <p><b><math>F_G</math></b> Fissure fill, formed in Event G; faulted in 1906; chaotic pebble-cobble gravel</p> | <p><b>FZ</b> Sheared gravel, silt and sand in fault zone</p> <p><b>50</b> Channel complex; loose, poorly sorted, matrix-supported, pebble gravel in coarse sand matrix; massive to crudely bedded</p> <p><b>60</b> Brown, massive, sandy silt, with scattered pebbles and abundant charcoal</p> <p><b>70</b> Channel complex; loose, poorly sorted, massive, matrix- to clast-supported, cobble gravel in coarse sand-pebble matrix</p> | <p><b>100</b> Grey, mottled sandy silty clay to clayey silty sand with scattered pebbles and sparse large clasts; clasts deeply weathered; hatchures mark change in color from dark grey above to orange mottled below</p> <p><b>▲</b> 1163-1259 AD Radiocarbon sample location with calibrated age.</p> <p><b>—</b> Most recent event (1906?) fault traces</p> <p><b>—</b> Penultimate event ("event G") fault traces</p> <p>"K" indicates krotovina<br/>Light line weight contacts mark lenses of different material within numbered unit</p> |
|--|---|---|

Figure 8. Log of northwest wall of Trench T1. Late Holocene coarse-grained channel and fine-grained overbank deposits are displaced by multiple near-vertical to steeply dipping fault strands. Stratigraphic and structural relations provide evidence for two ground rupturing events: (1) the MRE (presumably 1906) is expressed by fault strands (shown in red) approaching the ground surface and terminating in a heavily bioturbated zone. The fault terminations are overlain by a colluvial wedge ( $R_{1906}$ ) composed of gravelly rubble raveled off the 1906 scarp face; (2) The penultimate event (Event G) represents the displacement of the lower part of unit 40 across several fault strands (shown in purple). Event G exposed units 50, 60 and 70, generating cobbly colluvium that appears as a few scattered cobbles within the lower part of unit 40. Event G also produced a fissure ( $F_G$ ), which was subsequently faulted in 1906. Deposition of unit 40 overbank silts continued after Event G.

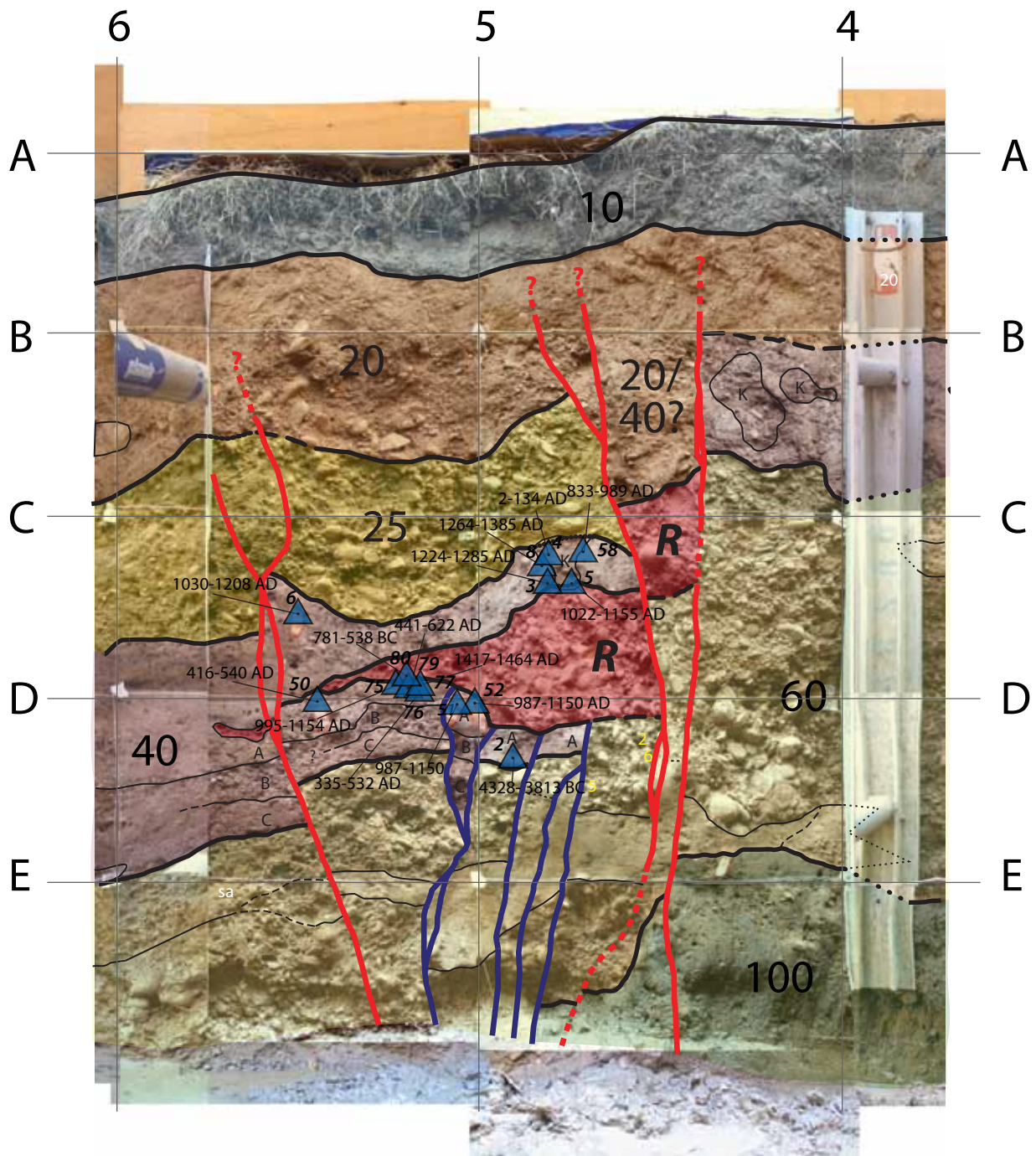


Figure 9. Close-up of the fault zone in the southeastern wall of Trench T2. Several charcoal samples from the overbank silts (unit 40) that pre-date and post-date the colluvial wedge “R” formed after Event G were dated to provide constraints on the age of the event. Sample locations are marked with blue triangles, with sample number and calibrated date range indicated. Results are tabulated in Table 1. See Figure 7a for explanation of units.